Characterization and Magnetic Properties of Nanoparticle $Ni_{1-x}Zn_xFe_2O_4$ Ferrites Prepared Using Microwave Assisted Combustion Method

Manoj M. Kothawale, R. B. Tangsali, G. K. Naik & J. S. Budkuley

Journal of Superconductivity and Novel Magnetism
Incorporating Novel Magnetism

ISSN 1557-1939
Volume 25
Number 6

J Supercond Nov Magn (2012)
25:1907-1911
DOI 10.1007/s10948-012-1510-8

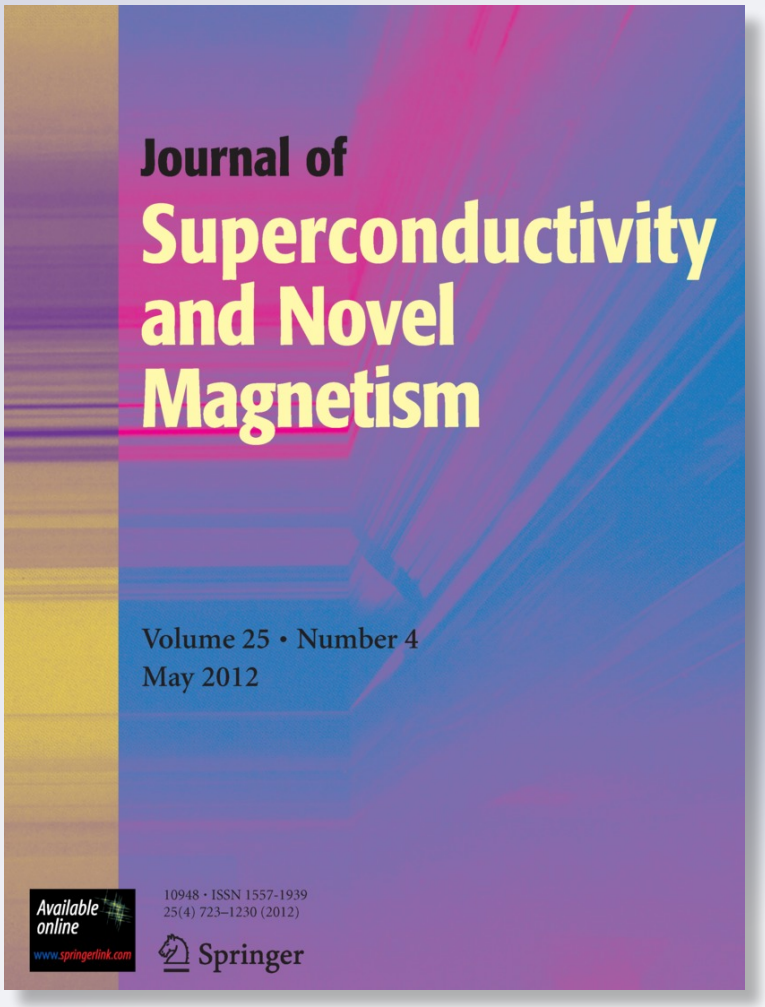

Springer

J Supercond Nov Magn (2012) 25:1907–1911
DOI 10.1007/s10948-012-1510-8

ORIGINAL PAPER

Characterization and Magnetic Properties of Nanoparticle $Ni_{1-x}Zn_xFe_2O_4$ Ferrites Prepared Using Microwave Assisted Combustion Method

Manoj M. Kothawale · R.B. Tangsali · G.K. Naik · J.S. Budkuley

Published online: 18 March 2012

Abstract Nanoparticle $Ni_{1-x}Zn_x$ Fe_2O_4 ($x = 0.35, 0.45$) samples were prepared successfully via microwave assisted combustion method. Synthesis of nanosize materials at a low temperature using a domestic microwave oven is the unique feature of this method and is being tried for the first time to produce NiZn ferrites. Single-phase formation of the samples was confirmed from X-ray analysis and IR spectrum. XRD data reveals that lattice parameter increases with Zn content 'x'. Particle sizes calculated from XRD analysis are in good agreement with TEM results. Extent of spin canting at octahedral B-site is deduced from Yafet–Kittel angles. Surface properties and reduced particle size affects the Curie temperature.

Keywords Ni–Zn ferrites · XRD · TEM · Magneton number · Saturation magnetization · Curie temperature

M.M. Kothawale (✉)
Department of Physics, D.M.S. College of Arts Science and Commerce, Assagao, Goa 403 507, India
e-mail: manojkothawale@yahoo.com

R.B. Tangsali
Department of Physics, Goa University, Taleigao Plateau, Goa 403206, India
e-mail: rbtangsali@unigoa.ac.in

G.K. Naik
Department of Chemistry, S.P.C. College of Arts and Science, Margao, Goa, India

J.S. Budkuley
Department of Chemistry, Goa University, Taleigao Plateau, Goa 403206, India

1 Introduction

Spinel ferrites are technologically important class of magnetic oxides because of their magnetic properties, high electrical resistivity, low eddy current and low dielectric loss, high Curie temperature, high permeability, etc. [1]. Among the soft ferrites, Ni-Zn ferrites are of commercial importance due to their high frequency applications in different devices such as radio frequency coils, transformer cores, etc. [2]. Owing to impact of fine particles on properties of Ni-Zn ferrites and considering its possible consequent effects on the technological applications, synthesis of solids possessing desired structures, stoichiometry and properties continues to be a real challenge for researchers. Various wet chemical methods involving synthesis of metal and mixed metal oxides using metal hydrazine complexes of oxalate, malonate, succinate, maleate, tartrate, and fumarate, etc. have been developed [3]. In the present paper, it is decided to do study of magnetic properties of nanoparticle Ni-Zn ferrites prepared using microwave assisted combustion method. This method yields NiZn nanoferrites at low temperature. Synthesis of ZnO, cadmium substituted lithium ferrites, etc. via microwave assisted combustion method using domestic microwave oven has been already reported [4].

2 Experimental

Calculated amount of raw materials namely ferrous nitrate, nickel nitrate, and zinc nitrate (all salts of AR grade) in stoichiometric proportions were dissolved in double distilled water and mixed thoroughly using magnetic stirrer. This mixture was then added to a solution containing appropriate amount of nitrilotriacetic acid and hydrazine hydrate (both AR grade). The precursor solution was then heated

and stirred using a conventional magnetic stirrer. Heating of the solution was continued, until mixture gets converted into a thick paste resulting in to a solid sticky mass. The solid sticky mass was collected in a crucible and then decomposed using domestic (600 W, 2.4 GHz) microwave oven. The sample is obtained in the form of residue after combustion. The powder obtained was thoroughly ground in an agate mortar and used for characterization. The X-ray powder diffraction patterns were recorded on a Rigaku X-ray diffractometer using CuKα radiation and 2θ scanning range from 20° to 80°. IR spectra for all the samples were recorded using Shimatzu Fourier transform infrared (FTIR) 8900 spectrometer in the range of range of 300 cm^{-1} to 1000 cm^{-1}. Samples were prepared in the form of pallets with KBr to specimen ratio as 1:100 for IR measurements. Transmission electron microscope (TEM) images were recorded on Hitachi H7500 transmission electron microscope. Saturation magnetization, coercivity, and retentivity at room temperature were measured using automated high field Hysteresis loop tracer. The low field A.C. susceptibility measurements in the temperature range 300–800 K were done using Likhite's automated double coil set up.

3 Results and Discussion

3.1 XRD Analysis

The X-ray diffraction (XRD) patterns for the samples of $Ni_{1-x}Zn_xFe_2O_4$ for $x = 0.35$ and 0.45 are shown in Fig. 1. The strongest refection coming from the (311) plane denotes the spinel phase. The positions of the peaks comply with reported ones in JCPDS file no 8-234 and AMCSD

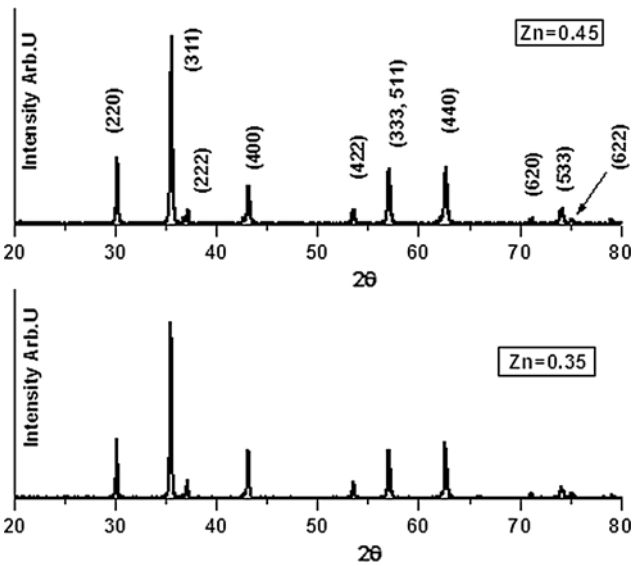

Fig. 1 XRD patterns for $Ni_{1-x}Zn_xFe_2O_4$

card 99-101-2527. This confirms that samples under study are having single phase cubic spinel structure. Exact lattice parameter for each samples were calculated using Nelson–Riley method [5]. The values of lattice constant 'a' are in good agreement with reported literature [2]. It is observed that lattice parameter increases with increasing Zn concentration. The increase in 'a' can be explained on the basis of the ionic radii, i.e., Zn^{2+} (0.74 Å) > Ni^{2+} (0.69 Å) [5, 6]. Also, an increase in lattice constant with increasing Zn content confirms the formation of compositionally homogeneous samples. The crystallite size of the nanocrystalline samples were calculated using the Debye–Scherrer formula given in Eq. (1).

$$D = 0.89\lambda/\beta\cos\theta \tag{1}$$

where D is the crystallite size in nm, λ is the X-ray wavelength in Å, β is the line broadening at full width half maxima intensity (FWHM) in radians, and θ is Bragg angle. Average crystallite sizes were calculated for seven major reflections (220), (311), (222), (400), (422), (511), and (440) from XRD.

Average crystallite size $D = 45$ nm pattern of each sample (see Table 1). Average crystallite size for Zn = 0.45 was found to be 45 nm. TEM image and particle size distribution for Zn = 0.45 is shown in Fig. 2 and Fig. 3, respectively. TEM results of particle sizes are in agreement with crystallite sizes obtained from XRD data.

3.2 IR Analysis

IR absorption spectra of samples show two absorption bands as shown in Fig. 4. The higher band ν_1 is between wave number 600–550 cm^{-1} whereas lower band ν_2 between 450–385 cm^{-1}. This is a common feature of all the ferrites indicating single phase spinal structure having two sublattices [5, 7–9].

The highest band ν_1 corresponds to intrinsic stretching vibrations of metals at the tetrahedral site, M_{tetra}–O, whereas lowest band ν_2 is assigned to octahedral metal stretching, M_{oct}–O. The ν_2 band values are less compared to that of

Table 1 Miller indices (hkl), full width half maxima of peaks (FWHM), Bragg's angle (2θ) and crystallite size using Scherrer equation for nocrystalline $Ni_{0.55}Zn_{0.45}Fe_2O_4$

hkl	FWHM deg	2θ deg	Crystallite size nm
220	0.166	30.10	49
311	0.170	35.45	48
222	0.144	37.12	58
400	0.182	43.09	46
422	0.188	53.42	47
333	0.274	56.94	32
440	0.246	62.53	37

Table 2 Zinc concentration (x), lattice constant (a), average crystallite size (D), saturation magnetization (Ms), coercivity (Hc), retentivity (Mr), observed and theoretical magneton number (n_{Bobs} and n_{Bth}), Yafet–Kittel angle (θ_{YK}) and Curie temperature (T_{C}) for $Ni_{1-x}Zn_XFe_2O_4$ nanoferrites

Zn (x)	a (Å)	D nm	Ms emu/g	Hc Oe	Mr emu/g	n_{B} obs μ_{B}	n_{B} th μ_{B}	θ_{YK} deg	T_{C} °C
0.35	8.3839	56	73	58	5.3	3.098	4.8	38°	474
0.45	8.3855	45	79	61	4.5	3.123	5.6	45°	480

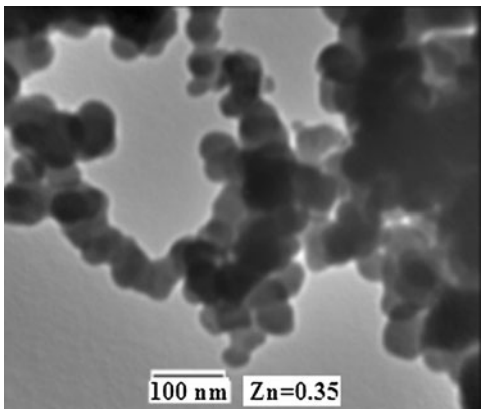

Fig. 2 TEM image for $Ni_{0.55}Zn_{0.45}Fe_2O_4$

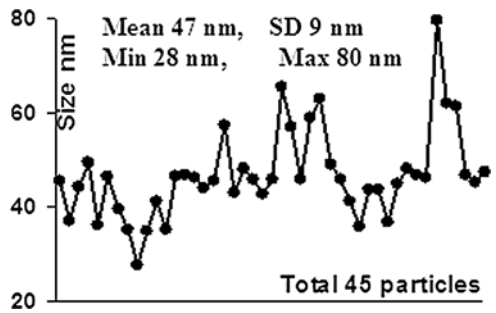

Fig. 3 Particle size distribution derived from TEM image for $Ni_{0.55}Zn_{0.45}Fe_2O_4$

the ν_1 band. This is due to the fact that the tetrahedral site dimension is less compared to the octahedral site dimension.

3.3 Magnetic Measurements

The saturation magnetization (Ms) and the magneton number (n_{B}) increases with Zn concentration. Similarly is the report by Jadhav et al. [2] for $x < 0.40$ and Kakatkar et al. [10] for $x < 0.30$ in case of NiZn ferrite prepared by the standard ceramic method. The net magnetization of the sample is given by $M = M_{\mathrm{B}} - M_{\mathrm{A}}$, where M_{A} and M_{B} are the magnetic moments of A and B sites, respectively. Substitution of Zn (Zn ion prefers A site) will lead to an increase in Fe^{3+} ions on B site, and hence B site magnetization. At the same time, the magnetization of the A site will decrease due to a decrease in Fe^{3+} ion on A site. Thus, net magnetization will increase with increase in Zn content. Even

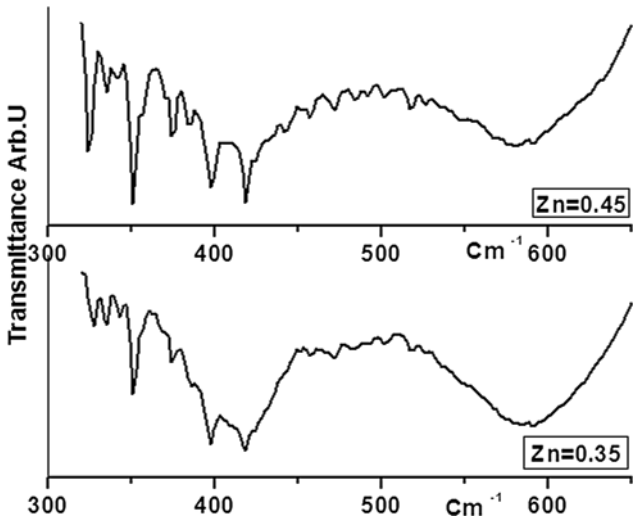

Fig. 4 IR spectrum for $Ni_{1-x}Zn_xFe_2O_4$

though a replacement of a magnetic Ni^{2+} ion by a non-magnetic Zn^{2+} ion leads to decreases in A–B interaction, the net difference of magnetic moment between A and B site ion increases showing increase in saturation magnetization Ms, and magnetic moment n_{B}. The observed value of (Ms) for $x = (0.35, 0.45)$ are found to be higher compared to some reported results [2, 10] which may be due to a microwave assisted decomposition technique used in preparing these samples. The magnetic parameters such as saturation magnetization, coercivity, and retentivity are given in Table 2. Samples also shown for low hysteresis loss, low coercivity, and low retentivity. Magnetic hysteresis loops for $Ni_{1-x}Zn_xFe_2O_4$ samples are shown in Fig. 4.

Calculation of magneton number (saturation magnetization per formula unit) was done based on the site preferences of the ions in NiZn ferrites and on cation distribution reported in the literature [11]. Discrepancies in the observed and theoretical magneton number indicate that significant canting exists at B-site. This suggests that the magnetic structure is non-collinear. Yafet–Kittel angles were found to be increasing with Zn content (see Table 2).

Preparation method, chemical composition, microstructure, and grain size plays crucial role in deciding magnetic susceptibility. Thermal variation of magnetic moment for the samples $x = 0.35$ and 0.45 is as shown in Fig. 5 and can be used to determine Curie temperature (given in Ta-

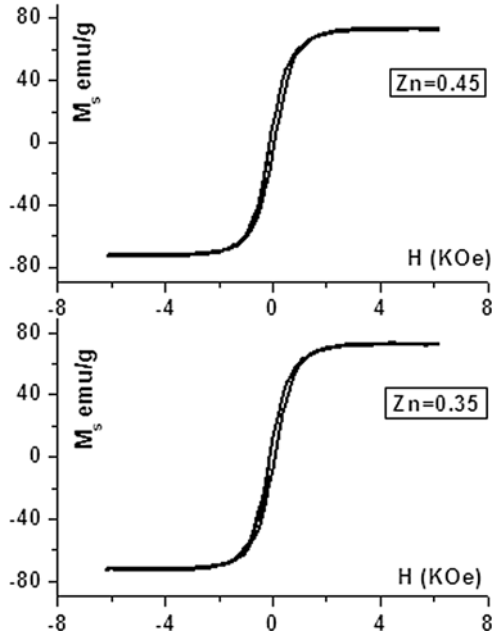

Fig. 5 Magnetic Hysteresis loops for $Ni_{1-x}Zn_xFe_2O_4$

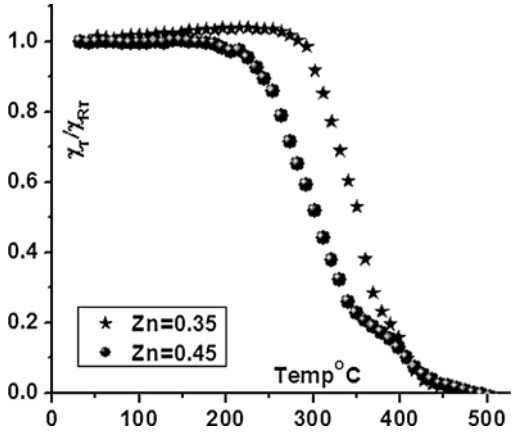

Fig. 6 Variation of normalized susceptibility with temperature for $Ni_{1-x}Zn_xFe_2O_4$

ble 2). It is a known fact that Curie temperature generally goes on decreasing with the addition of non-magnetic zinc ions. This is attributed to a decrease in A–B interaction resulting from the replacement of magnetic Fe^{3+} by non-magnetic Zn^{2+} ion. According to Neel's model, A–B interaction is most dominant in ferrites and Curie temperatures of the ferrites are determined from overall strength of A–B interaction. Strength of A–B interaction is a function of number of $Fe_A{}^{3+}$–O^{2-}–$Fe_B{}^{3+}$ linkages, which, in turn, depends upon number of Fe^{3+} ions in the formula unit and their distribution amongst tetrahedral (A) and octahedral [B] sites. In this system, Ni^{2+} (2 μB) ions are replaced by Zn^{2+} (0 μB). This results in a decrease of A–B interaction, which may lead to decrease in Curie temperature (T_C). However, in present case, there is slight increase in T_C with increase in Zn, which is unexpected. It can be seen from Fig. 6, the rate of decrease in magnetic moment for $x = 0.45$ slows down after 350 °C. As temperature approaches to T_C, it further slows down compared to that of $x = 0.35$. This leads to increase in T_C of sample $x = 0.45$ compared to $x = 0.35$. This effect is attributed to particle size, particle shape, and lattice fluctuations. The magnetic properties of nanoparticles are found to be affected by both particle shape and lattice fluctuations [8, 12]. To study Curie temperature, surface properties such as number of surface atoms, variations in exchange coupling of surface atoms, and lattice fluctuations should be considered. Particle shapes are important for T_C estimations because it determines the number of surface atoms whose reduced coordination number affects the exchange energy locally. Lattice fluctuations are also important because they increase with temperature and have an impact on Heisenberg exchange. Also, smaller particles are expected to have relatively large thermally induced fluctuations of the lattice. Note that in our case particle size for $x = 0.45$ is less compared to $x = 0.35$. Thus residual magnetization near Curie temperature may be arising due to their small sizes. In a small system, exchange interaction is strong enough to induce short-range correlations of the moments even at temperatures higher than T_C of the main phase. As the size of the system is reduced to values close to correlation length it becomes more difficult for the system to achieve zero net magnetization and in these cases correlations are completely destroyed at temperature much greater than T_C of the main phase. This effect may lead to broadening of the ferromagnetic transition. Broadening of the ferromagnetic transition becomes more pronounced as the particle sizes are reduced. Thus, higher T_C for $x = 0.45$ may be attributed to small particle size effect.

4 Conclusions

Nanoparticle $Ni_{1-x}Zn_xFe_2O_4$ for $x = 0.35$ and 0.45 was prepared at low temperature via microwave assisted combustion method using domestic microwave oven. Average particle sizes were found to be 45 nm, 56 nm for Zn = 0.45, Zn = 0.35, respectively. Lattice parameter increases with increasing Zn concentration. Variation of magnetic moment (n_B) with Zn content is not governed by two sub-lattice models and a magnetic structure is non-collinear with significant spin canting at B-site. Yafet–Kittel angles increases with Zn concentration. The residual magnetization near Curie temperature and broadening of the ferromagnetic transition may be arising from surface properties and reduced particle size.

References

1. Pandit, A.A., More, S.S., Dorik, R.G., Jadhav, K.M.: Bull. Mater. Sci. **26**, 517–521 (2003)
2. Jadhav, S.S., Shirsath, S.E., Toksha, B.G., Shukla, S.J., Jadhav, K.M.: Chin. J. Chem. Phys. **21**, 381–386 (2008)
3. Porob, R.A., Khan, S.Z., Mojumdar, S.C., Verenkar, V.M.S.: J. Therm. Anal. Calorim. **86**, 605–610 (2006)
4. Das, S., Mukhopadhyay, A.K., Datta, S., Basu, D.: Bull. Mater. Sci. **32**, 1–13 (2009)
5. Akther Hossaina, A.K.M., Mahmuda, S.T., Seki, M., Kawai, T., Tabata, H.: J. Magn. Magn. Mater. **312**, 210–219 (2007)
6. Mona, M.B., Sarah, B., Octavio, P.: J. Solid State Chem. **178**, 1080–1086 (2005)
7. Ayer, R., Desai, R., Upadhay, R.V.: Bull. Mater. Sci. **32**, 141–147 (2009)
8. Ayer, R., Desai, R., Upadhay, R.V.: Indian J. Pure Appl. Phys. **47**, 180–185 (2009)
9. Ladgaonkar, B.P., Kolekar, C.B., Vaingankar, A.S.: Bull. Mater. Sci. **25**, 351–358 (2002)
10. Kakatkar, S.V., Kakatkar, S.S., Patil, R.S., Sankpal, A.M., Suryawanshi, S.S., Bhosale, D.N., Sawant, S.R: Phys. Status Solidi (b). Basic Solid State Phys. **198**, 853–860 (1996)
11. Patil, S.A., Bhise, B.V., Ghatage, A.K.: Mater. Chem. Phys. **65**, 38–42 (2000)
12. Evansa, R., Nowak, U., Dorfbauer, F., Shrefle, T., Mryasov, O., Chantrell, R.W., Grochola, G.: J. Appl. Phys. **99**, O8G701 (2006)